



Identification of Elevated Aerosol Layers and their properties by using ground-based aerosol measurements over the foothills of the central Himalayas

Amit Singh Chandel^{*①}, Chandan Sarangi^{# ①}, Rakesh Hooda^②, and Antti Hyvärinen^②

(1) Indian Institute of Technology Madras, Chennai, India

(2) Finnish Meteorological Institute, Helsinki, Finland

Abstract

Previous studies have identified and examined the elevated aerosol layers (EAL) using LiDAR measurements from CALIPSO or MPLNET. Here we identify the EALs and their properties using ground-based aerosol measurements in Mukteshwar, a remote site in the Himalayan Mountains in northern India, from 2006–2013 (March-August only). EAL events are screened from the 8-year measurements by considering the ratio of PM₁₀ to PM_{2.5} equal to or greater than two. BC increases by two to threefold and shows a good association with the PM concentration during the EAL events. The presence of strongly absorbing and scattering aerosol in EAL can be seen by their varying range of 10-50 Mm⁻¹ and 50-350 Mm⁻¹, respectively. CALIPSO, MPLNET, Dust Aerosol Optical Thickness, and NASA'S Worldview Earthdata are used to verify the EAL events identified from the ground-based aerosol measurements. The back-trajectory analysis clearly shows an influx of air mass from Arabia's arid regions and the west Arabian sea.

1. Introduction

As a result of scattering and absorption of incoming and outgoing radiation, the atmosphere's aerosols play a significant role in climate change by altering cloud properties, such as cloud droplet size distribution and cloud lifetime [1, 2]. Aerosol vertical profiles provide more insight into aerosol impacts on climate change, such as aerosol warming is responsible for the increased thermal stability and structure of the atmosphere, resulting from the presence of distinct layers of aerosol above the atmosphere coined as elevated aerosol layers (EALs) [3, 4]. The higher aerosol concentration is mainly confined within the atmospheric boundary layer (ABL), but sometimes they are overshoot to higher altitudes (2-4 Km) represented as EAL. EALs are mainly observed in the lower troposphere, influenced by vertical advection and wind speed. [5] reported that EALs are frequent over the Indian subcontinent during the pre-monsoon and are generally formed due to convective lifting and upper air long-range transport (LRT) from distant locations. [6] modelled the transportation of dust and reported that during pre-monsoon, dust is transported across the Indo-Gangetic Plain (IGP) at an elevation of 700-850 hPa and accumulates over the Himalayas. Cloud-Aerosol Lidar and Infrared Pathfinder Satellite Observations (CALIPSO) observations were used to investigate the vertical extent of the EALs over the central IGP and found the extent up to 4Km with maximum elevations in May [7, 8]. In another study [9], EALs were absorbed during pre-monsoon over Kanpur using ground-based lidar measurements. As all the studies related to EALs are mainly based on satellite observations and few in situ and aircraft measurements, more in-depth research is required to understand EAL further, its properties, and its effect on atmospheric processes. The atmospheric warming/cooling by the elevated aerosol layer (EAL) and its composition remain one of the unaddressed issues related to atmospheric aerosols. Understanding the nature of BC is essential for climate change because of its strong absorption over a wide range of wavelengths, combined with its smaller size (submicron) and longer lifetime in the atmosphere [10]. In this context, the present work deals with a hypothesis to indirectly identify the EAL events and their optical properties and one more interesting fact: BC increases with EAL events. In this perspective, the Thermo-Beta-Attenuation Mass Monitors, Aethalometer, Integrating Nephelometer, and Differential Mobility Particle Sizer (DMPs) are used to measure the particulate mass concentration (PM₁₀ & PM_{2.5}), BC concentration, and absorption

coefficient, scattering coefficient, and aerosol particle size distribution (10-800 nm) respectively. We use the ratio of PM10 and PM2.5 and the extinction coefficient to identify the EAL events.

2. Aerosol Instrumentation and Data Processing

This study proposes an indirect way to identify the EAL events and one more interesting fact: BC increases with EAL events. To conquer this, we used various aerosol measuring instruments with a temporal resolution of 5 minutes. Such as Thermo-Beta-Attenuation Mass Monitors to measure the particulate mass concentrations (PM2.5 and PM10), Magee Scientific AE-31 Aethalometer that has seven wavelengths (370 to 950 nm) to measure the absorption coefficients (σ_{ap}), and equivalent black carbons (eBC) at 880 nm. Scattering coefficients (σ_{sp}) were measured at 525 nm with an integrating nephelometer (Ecotech M 9003). The differential mobility particle sizer (DMPS, Finnish Meteorological Institute assembled) was used to measure particle size distribution. The DMPS data were categorized into three-size bins, namely Nucleation mode (Nnuc), Aitken mode (Nait), and Accumulation mode (Nacc), having a size ranging from 10-25 nm, 25-90 nm, and 90-800 nm, respectively. The sum of the particle number concentrations in the three particle size ranges is Ntot (Total number concentration of particles). The time series of aerosol measurements from September 2005 to January 2014 are analyzed. We confined our search to March to August only as EALs are mainly observed during these periods over the Indian subcontinent. We used CALIPSO data to examine the vertical extent of the aerosol layer and aerosol subtype to identify EAL events. NASA's Micro-Pulse Lidar Network (MPLNET) data (<https://mplnet.gsfc.nasa.gov/>) over Kanpur, Dust Aerosol Optical Thickness data (<https://gmao.gsfc.nasa.gov/>) and NASA'S Worldview Earthdata (<https://worldview.earthdata.nasa.gov/>) over India are used to identify the EAL events. Aerosol instrument data are analyzed for the confirmed dates of EAL events. The pattern observed from the above-confirmed event data was used as an input to identify more EAL events from the aerosol instrument's data. The events are identified based on PM10 and PM2.5 ratios equal to or greater than two. The extinction coefficient is the sum of absorption and scattering coefficients and is used to verify the EAL event identified based on PM10 and Pm2.5 ratios and examine EAL's nature. The EAL event ranged from 3-7 days. For each EAL event observed, we took 4-5 days before and after the EAL event (subject to availability) as the background observation (Pre EAL). Time series of the event (EAL & Pre EAL) were also matched with time series of BC and absorption and extinction coefficients. A total number of 22 EAL events was identified, out of which results from 4 of them are focused here.

3. Results and Discussion

EALs are mainly identified by analyzing the vertical distribution of aerosol layers measured by LIDAR onboard CALIPSO satellite or ground-based NASA's Micro-Pulse Lidar Network (MPLNET). Analyzing data from 2006 to 2013, we got 30 EAL days observed by CALIPSO over the study location (~100 Km²); when restricting from March to August, we got 12 EAL days (event). From all the 12 events, we could analyze the aerosol measurements data for only four events due to the unavailability of data for other dates observed by CALIPSO. The Worldview Earthdata and data from MPLNET (subject to availability) also supported the presence of EAL over the study region for all the identified events. Confirmation of the EAL events over the study region is shown in Figure 1 as observed by MODIS (Figure 1 a) and CALIPSO (Figure 1 b). It is pretty discernible from Figure 1 that during an EAL event, there is an increment in both PM10 and PM2.5 concentrations, and the ratio of PM10 to PM2.5 is equal to or greater than two, as proposed by us to identify EAL events by ground-based measurements. From the time series of PM, BC, number mass concentration, absorption, scattering, and extinction coefficients, we found that all aerosol measurements increased by 2-3 folds during EAL events compared to Pre EAL days. It is well-known that many bigger particles, e.g., dust, are present in the atmosphere, reducing the incoming solar radiation by mostly scattering light during EAL. Due to EAL, the extinction of light may be up to two to threefold, as stated by Satheesh et al., 2008. Table 1 shows the increment of aerosol optical and microphysical properties during the EAL event and the corresponding increase in the BC concentration. It can be inferred from the table that, apart from an increase in scattering coefficient, likely due to increasing dust concentration during EAL, the absorption coefficient is also increasing similarly. The increasing absorption coefficient may be due to BC and BrC (brown carbon) increment during the EAL event. Although the contribution of the absorption coefficient in calculating the extinction coefficient is significantly less (~10%, as observed by this study), it plays a significant role in modifying the atmospheric dynamics. The absorptive nature of EAL, when in contact with the snow or ice, may cause surface warming resulting in the melting of snow and ice at a greater rate.

Analyzing the microphysical properties of aerosol particles for the selected example reveals more increment in the smaller size particles (Nait) compared to the larger particles (Nacc), indicating more anthropogenic pollution. Although the mass concentration of smaller particles compared to the larger size particles will be significantly less, its effect on optical properties will be more due to the large surface area resulting from the increasing number of particles. The peak of the optical properties along with BC concentration is mainly observed from afternoon to

evening (1300hrs - 2000hrs) slightly more towards the evening time, indicating the layers to be well mixed. As time progresses, the planetary boundary layer (PBL) height also decreases, resulting in the high concentration of pollutants near the surface (sensors of the aerosol measurements) as recorded by the sensors. To check if the conclusions made from the four examined EAL events were correct or not, we used the conclusion as a screening tool to identify the other EAL events for which we did not have visual confirmation. We could get only 22 such EAL events from the 8-year aerosol measurement data because, most of the time, the instruments were in maintenance. However, we got satellite confirmation only for some EAL events as CALIPSO is limited in temporal resolution of 16 days, and MODIS can not screen clouds very well. The resulting changes in aerosol microphysical and optical properties during the EAL and Pre EAL days for 22 events will be discussed in the future.

4. Figures and Tables

4.1 Figures

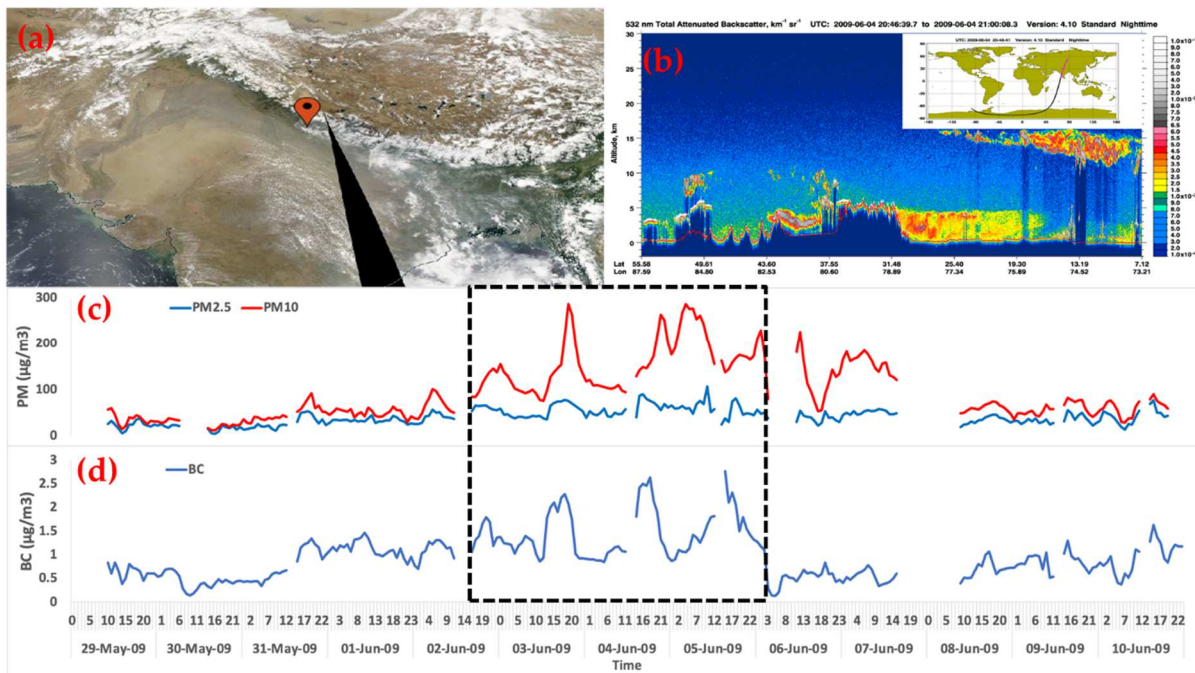


Figure 1. A typical example showing an EAL event by MODIS (Figure 1 a) and from CALIPSO (Figure 1 b) during 20:46-21:00 UTC on 4th June 2009. Figure 1 (c) & (d) shows the time series of PM10, PM2.5, and BC concentrations respectively. The black colour dashed line box indicates the EAL event period.

4.2 Tables

Table 1. Aerosol properties and meteorological parameters for the four identified EAL events

Aerosol Property	21-Mar-12			25-May-06			19-May-12			04-Jun-09		
	Pre_EAL	EAL	Post_EAL									
BC ($\mu\text{g}/\text{m}^3$)	1.12	1.67	0.86	0.73	1.49	1.03	1.85	3.47	1.41	0.79	1.45	0.72
PM2.5 ($\mu\text{g}/\text{m}^3$)	45.26	61.96	42.38	26.69	46.26	26.72	43.63	117.73	46.58	28.18	56.73	39.56
PM10 ($\mu\text{g}/\text{m}^3$)	98.06	162.50	81.95	51.75	120.02	49.85	79.27	343.24	102.84	44.71	157.26	87.55
PM10/PM2.5	2.23	2.55	2.02	2.04	2.53	1.88	1.95	2.78	2.39	1.64	2.85	2.19
σ_{sp} (Mm^{-1})	91	123	65	61	133	76	126	249	117	76	132	73
σ_{ap} (Mm^{-1})	15	22	12	10	19	13	30	53	24	9	19	11
σ_{ext} (Mm^{-1})	105	145	77	71	152	90	156	302	141	85	151	83
N_{tot} (cm^{-3})	4449	5562	4476	2239	3421	2468	6577	7966	6432	3468	5910	4791
N_{nuc} (cm^{-3})	114	318	103	23	34	40	45	37	74	166	293	485
N_{ait} (cm^{-3})	1968	2313	2211	911	1292	974	2083	2221	2239	1729	3173	2621
N_{acc} (cm^{-3})	2367	2931	2162	1305	2096	1453	4448	5708	4119	1573	2444	1685
Press (hPa)	785	784	784	781	781	781	781	783	783	780	779	779
Rad (Wm^{-2})	212	201	272				270	201	277	137	153	147
RH (%)	33	44	18	85	86	82	34	45	27	72	57	29
Temp ($^{\circ}\text{C}$)	16	14	17	17	18	18	19	19	20	15	21	21

7. References

1. Ackerman, A. S., Toon, O. B., Stevens, D. E., Heymsfield, A. J., Ramanathan, V., & Welton, E. J. (2000). Reduction of tropical cloudiness by soot. *Science*, 288(5468), 1042-1047.
2. Twomey, S. J. A. E. (1974). Pollution and the planetary albedo. *Atmospheric Environment* (1967), 8(12), 1251-1256.
3. Padmakumari, B., Maheskumar, R. S., Harikishan, G., Morwal, S. B., Prabha, T. V., & Kulkarni, J. R. (2013a). In situ measurements of aerosol vertical and spatial distributions over continental India during the major drought year 2009. *Atmospheric environment*, 80, 107-121.
4. Prabha, T. V., Karipot, A., Axisa, D., Kumari, B. P., Maheskumar, R. S., Konwar, M., ... & Goswami, B. N. (2012). Scale interactions near the foothills of Himalayas during CAIPEEX. *Journal of Geophysical Research: Atmospheres*, 117(D10).
5. Sarangi, C., Tripathi, S. N., Mishra, A. K., Goel, A., & Welton, E. J. (2016). Elevated aerosol layers and their radiative impact over Kanpur during monsoon onset period. *Journal of Geophysical Research: Atmospheres*, 121(13), 7936-7957.
6. Das, S., Dey, S., Dash, S. K., & Basil, G. (2013). Examining mineral dust transport over the Indian subcontinent using the regional climate model, RegCM4. 1. *Atmospheric research*, 134, 64-76.
7. Gautam, R., Hsu, N. C., Lau, K. M., & Kafatos, M. (2009, September). Aerosol and rainfall variability over the Indian monsoon region: distributions, trends and coupling. In *Annales Geophysicae* (Vol. 27, No. 9, pp. 3691-3703).
8. Mishra, A. K., & Shibata, T. (2012). Climatological aspects of seasonal variation of aerosol vertical distribution over central Indo-Gangetic belt (IGB) inferred by the space-borne lidar CALIOP. *Atmospheric Environment*, 46, 365-375.
9. Misra, A., Tripathi, S. N., Kaul, D. S., & Welton, E. J. (2012). Study of MPLNET-derived aerosol climatology over Kanpur, India, and validation of CALIPSO level 2 version 3 backscatter and extinction products. *Journal of Atmospheric and Oceanic Technology*, 29(9), 1285-1294.
10. Babu, S. S., Moorthy, K. K., Manchanda, R. K., Sinha, P. R., Satheesh, S. K., Vajja, D. P., ... & Kumar, V. A. (2011). Free tropospheric black carbon aerosol measurements using high altitude balloon: Do BC layers build "their own homes" up in the atmosphere?. *Geophysical research letters*, 38(8).